Molten Globule and Native State Ensemble of *Helicobacter pylori* Flavodoxin: Can Crowding, Osmolytes or Cofactors Stabilize the Native Conformation Relative to the Molten Globule?

N. Cremades and J. Sancho
Biocomputation and Complex Systems Physics Institute and Departamento de Bioquímica y Biología Molecular y Celular, Facultad de Ciencias, Universidad de Zaragoza, Zaragoza, Spain

ABSTRACT Partly unfolded protein conformations close in energy to the native state may be involved in protein functioning and also be related to folding diseases, but yet their structure and energetics are poorly understood. One such conformation, the monomeric and well-behaved molten globule of *Helicobacter pylori* apoflavodoxin, is here investigated to provide, in a wide pH interval, a complete thermodynamic description of its unfolding equilibrium and the equilibrium linking molten globule and native state. All thermodynamic and molecular properties of the molten globule here analyzed are characteristic of a partly unfolded conformation, and their differences with those of the native state are typically quantitative rather than qualitative. The stability data depict a native state ensemble where the relative populations of the different intermediates are strongly modulated by pH. Whereas the molten globule is dominant at pH 2.0, at neutral pH it is just the least stable of three partly unfolded intermediates populated by this protein. It is of interest that the energy rank of these intermediates at pH 7.0 is consistent with their likelihood to overcome the native state and become the more stable conformation when the native state protein is subjected to heat or mutation stress. Given the small volume difference between molten globule and native state, neither crowding agents nor osmolytes can drive the molten globule back to the native state. This observation, which is in qualitative accord with predictions of simple excluded volume theory, indicates that molecular crowding in vivo is not an effective mechanism to minimize partial unfolding events leading to equilibrium intermediates.

INTRODUCTION

It has been suggested that partly unfolded conformations of proteins that are close in energy to the native state under native conditions are relevant for protein function and in the onset of protein conformational defects (1,2). At this time, NMR techniques, such as hydrogen exchange dynamics, have been used to detect and characterize partly unfolded forms (PUFs) in the native ensemble (3–5). Classical thermodynamic analysis of partly unfolded forms arising under a variety of solution stress conditions can also shed light on the structure and energetics of these conformations and help to define native state ensembles. In this respect, global analysis of thermal unfolding equilibria (6,7) can provide good estimations of free energy differences between native and partly unfolded conformations, and can even delineate low-resolution structures of intermediates (6,8,9). One partly unfolded form of proteins, the molten globule, has received much attention due to its fascinating spectroscopic properties and to proposals that have implicated it in a variety of functional roles, such as protein folding (10,11) and protein membrane translocation (12,13). Yet, it is still difficult to know whether molten globules belong to native state ensembles at neutral pH or whether molten globules or other partly unfolded forms can respond to native stabilizing conditions, such as crowding, osmolytes, or cofactor binding, in the same fashion as native states. The fact is that although the stability of molten globules against full unfolding has been investigated over the years, less is known about the relative stability of native and molten globule conformations of proteins.

We use here the flavodoxin from the pathogenic bacteria *Helicobacter pylori* to investigate these issues. *H. pylori* is the only living entity, to our knowledge, able to survive in the human stomach, which is because of the presence of an H^+-stimulated cytoplasmic urease (14,15). The cytoplasmic pH of *H. pylori* has been proposed to vary between 8 and 5 depending on external pH and urea concentration in the medium (16–18). Since fluctuations in pH and urea concentration might exert a strong influence on the relative populations of the native state ensemble (2), it is possible that the bacteria use in vivo stabilizing mechanisms, such as macromolecular crowding or osmolytes, to counterbalance potential transient destabilizations of the native state. Flavodoxins are electron transfer proteins involved in many different reactions (19). *H. pylori* flavodoxin shuttles electrons from pyruvate to $NADP^+$ in an electron transport pathway specific for epsilon-proteobacteria (20). It has high sequence and structure homology with other members of the flavodoxin family (21,22) but a more exposed flavin mononucleotide (FMN) binding pocket due to the presence of an alanine residue where a conserved tryptophan is typical for most flavodoxins. This feature, which is being exploited to

Submitted January 24, 2008, and accepted for publication March 5, 2008.

Address reprint requests to J. Sancho, Departamento de Bioquímica y Biología Molecular y Celular, Facultad de Ciencias, Universidad de Zaragoza, Zaragoza, Spain. E-mail: jsancho@unizar.es

Editor: Doug Barrick.

0006-3495/08/08/1913/15 $2.00

doi: 10.1529/biophysj.108.130153

target new specific inhibitors for *H. pylori* eradication (23), makes the affinity for the FMN cofactor the lowest we have found for a long-chain flavodoxin ($K_d = 4.4$ nM at pH 7.0). Stability studies have demonstrated that *H. pylori* apoflavodoxin has both the highest stability toward full thermal unfolding and the lowest cooperativity (with two partially unfolded intermediates) we have yet observed for flavodoxins (24). Recently, we reported that at pH 2.0, it also populates a monomeric, partially unfolded conformation with molten globule characteristics (25) that seems structurally different from the two thermal intermediates identified at neutral pH. A similar conformation was described at acidic pH for the apoflavodoxin from *Anabaena,* which could not be characterized because it was not monomeric (26). However, a truncated version exhibiting molten globule characteristics at neutral pH was investigated by equilibrium phi-analysis (8,27) and was shown to be homogenously expanded and to display a nativelike secondary structure. Very little is known of the energetics of the equilibrium between the molten globule of *H. pylori* apoflavodoxin and the native state of known crystal structure (21,22) and dominant at neutral pH (25).

Since the apoflavodoxin molten globule is monomeric and unfolds in a reversible manner (25), it constitutes an interesting model to investigate molten globule energetics, and to determine whether molten globules belong to the cohort of partly unfolded conformations, close in energy to the native one, that form the native state ensemble (2,28). In addition, it provides a means to investigate whether common natural mechanisms that are known to stabilize native proteins against full unfolding are similarly effective to stabilize and recover functional native states in conditions where partially unfolded conformations become populated. According to our analysis, *H. pylori* flavodoxin remains functional between pH 2.0 and 10.0 thanks to the strong, native-specific ability of the FMN cofactor to bind to the native state, which compensates for the fact that at low pH the molten globule becomes more stable than the native conformation of the apoprotein. However, neither crowding agents nor osmolytes can significantly stabilize the native state relative to the molten globule, which indicates that these physiological mechanisms are not effective to minimize partial unfolding events leading to intermediates in the cell. A global analysis of all available thermodynamic information on the folding and binding equilibria, using data presented here combined with those from previous studies (24,25), has allowed us to delineate the dynamics of the free energy landscape of *H. pylori* flavodoxin along the pH axes. At neutral pH, the ensemble contains, in addition to the native state, the molten globule (this work) and two previously characterized equilibrium intermediates (24). Incidentally, the intermediate of the ensemble closer in free energy to the native state is the only one that has been observed to become dominant under mutational stress in the structurally homologous *Anabaena* flavodoxin (29,30).

MATERIALS AND METHODS

Recombinant expression and purification of *H. pylori* apoflavodoxin

Recombinant *H. pylori* flavodoxin was purified from a culture of *E. coli* cells (BL21) harboring the pET28a plasmid, which contains the flavodoxin gene (23). Apoflavodoxin was separated from holoflavodoxin in a MonoQ10 column (FPLC, Amersham, Piscataway, NJ), with a 0- to 1-M linear gradient of NaCl in Tris-HCl, pH 8. Apoflavodoxin was also obtained from holoflavodoxin by precipitation with trichloroacetic acid (31).

Spectroscopic characterization

UV fluorescence emission and far-UV and near-UV circular dichroism (CD) spectra were acquired at 25 ± 0.1°C at several pH values in both native and denaturing conditions (6 M urea or 90°C). Fluorescence emission spectra (300–400 nm, with excitation at 280 nm) were recorded in an Aminco-Bowman Series 2 spectrometer, and circular dichroism spectra in a Jasco 710 (Tokyo, Japan) or an Applied-Photophysics Chirascan (BioTools, Jupiter, FL) spectropolarimeter. Protein samples at different pH values were prepared by mixing concentrated buffer and protein solutions. Apoflavodoxin concentrations were 2–20 μM for fluorescence, 20 μM for far-UV CD, and 20–40 μM for near-UV CD experiments. All final buffer solutions were of 10 mM ionic strength. For fluorescence and near-UV CD, a cuvette of 1 cm pathlength was used, and for far-UV CD, a cuvette of 0.1 cm pathlength.

Urea-induced unfolding

The chemical stability of apoflavodoxin has been determined in the 1.5–5.0 pH interval, using urea as a denaturant. Protein samples (2 μM for fluorescence and 20 μM for far-UV CD) were prepared at the desired pH and urea concentration by mixing 900-μL urea solutions with 100-μL aliquots of buffered apoflavodoxin. The ionic strength of the different buffers in the final protein solutions was 10 mM. Protein samples were equilibrated at 25°C for at least 30 min before recording their spectroscopic signals. Unfolding curves were recorded throughout the 1.5–5.0 pH interval by emission fluorescence (ratio of 320/360 nm emission, with excitation at 280 nm). Additional unfolding curves were recorded at pH 2.0 and 5.0 by far-UV CD (at 222 nm) and at pH 5.0 by near-UV CD (at 291 nm). The influence of crowding on protein stability was determined by recording urea unfolding curves using protein samples that also contained dextran (35,000–45,000 average mol wt) (Sigma, St. Louis, MO) at a concentration of 100 mg/mL.

Unfolding data were analyzed as described (32,33), assuming a two-state equilibrium where the free energy of unfolding, ΔG, is considered to be a linear function of denaturant concentration, D:

$$\Delta G = \Delta G_W - mD, \tag{1}$$

where ΔG_w is the free energy of unfolding in buffered water and m is a proportionality constant. The spectroscopic signals of the folded and unfolded states (S_F and S_U at 0 M urea) are assumed to vary linearly with urea concentration; m_F and m_U are the corresponding slopes. Thus, the observed spectroscopic signal was fitted to

$$S = \frac{S_F + m_F D + (S_U + m_U D)e^{-(\Delta G_W - mD)/RT}}{1 + e^{-(\Delta G_W - mD)/RT}}, \tag{2}$$

where R is the gas constant and T the absolute temperature. At pH >2.0 and <4.0, both the native and molten globule states are significantly populated in the absence of urea. A three-state model (Eq. 3) was therefore used to fit the urea unfolding curves obtained in this pH interval.

$$S = \frac{S_N + m_N D + S_{MG} e^{-(\Delta G^W_{N-MG} - m_1 D)/RT} + (S_U + m_U D) e^{-(\Delta G^W_{MG-U} - m_2 D)/RT}}{1 + e^{-(\Delta G^W_{N-MG} - m_1 D)/RT} + e^{-(\Delta G^W_{MG-U} - m_2 D)/RT}}. \quad (3)$$

Individual fitting of the different curves obtained at a single pH value to the three-state model was unsatisfactory, because each of these curves shows an apparent two-state behavior. We thus performed a combined analysis of the curves obtained at pH 2.2, 2.6, and 3.17. In the analysis, the ΔG^W_{N-MG} value of each curve was previously calculated from a spectral deconvolution (see below) and fixed in Eq. 3. On the other hand, the m_1 and m_2 parameters, representing the urea dependencies of the free energies, were kept the same for the three pH values, since no significant changes are expected in the narrow 2.2–3.2 pH interval. To further reduce fitting dependencies, the unfolded state signal (S_U, m_U) was treated as a shared parameter for the three curves, whereas the slope of the signal of the intermediate state (i.e., the molten globule) was fixed at zero (34).

Thermal-induced unfolding

Thermal denaturation at pH 2.0 (in 23 mM sodium phosphate buffer) was assessed by fluorescence emission (emissions ratio 320/360 nm, which is proportional to the advance of the unfolding, because no change in intensity takes place at 360 nm (8)) and far-UV circular dichroism (222 nm) for apoflavodoxin. Apoflavodoxin concentration was 2–20 μM for fluorescence measurements and 20 μM for far-UV CD. Global fit of the spectroscopic unfolding curves of the apo form was performed assuming a two-state unfolding model,

$$S = \frac{S_N + m_N T + (S_U + m_U T) e^{-(\Delta G/RT)}}{1 + e^{-(\Delta G/RT)}} \quad (4)$$

with

$$\Delta G(T) = \Delta H_m (1 - (T/T_m)) - \Delta C_P ((T_m - T) + T \ln(T/T_m)), \quad (5)$$

where the spectroscopic signal of each state (S_N and S_U at $T = 0$) is supposed to vary linearly with temperature with slopes m_N and m_U, and ΔH_m, T_m, and ΔC_P are the enthalpy change at T_m, the melting temperature, and the heat capacity change of the transition, respectively.

For holoflavodoxin, the unfolding was also assessed by near-UV CD (291 nm) and absorbance at 291 nm. Holoflavodoxin was always used at 20 μM concentration. The clear nonsuperimposition of the unfolding curves monitored by different spectroscopic techniques suggested a three-state model for the equilibrium unfolding of the holoprotein. The equation used to globally fit the curves was

$$S = \frac{S_N + m_N T + (S_I + m_I T) e^{-\Delta G_1/RT} + (S_U + m_U T) e^{-(\Delta G_1 + \Delta G_2)/RT}}{1 + e^{-\Delta G_1/RT} + e^{-(\Delta G_1 + \Delta G_2)/RT}}, \quad (6)$$

where S_I and m_I are the signal of the intermediate state at $T = 0$ and its linear temperature dependency, whereas ΔG_1 and ΔG_2, the free energy differences of the native/intermediate and intermediate/unfolded equilibria, follow expressions analogous to the one in Eq. 5.

To obtain an accurate value for the unfolding heat capacity change of the molten globule, thermal unfolding at pH 2.0 was carried out in the presence of different urea concentrations (0, 0.4, 0.8, 1.0, 1.2, 1.4, and 3.0 M). A global fit of these curves was performed using a modified version of Eq. 4, assuming that S_N, m_N, S_U, and m_U show a linear dependence of urea concentration and that the free energy of unfolding follows:

$$\Delta G(T, D) = \Delta G(T) - f(D, T), \quad (7)$$

where $\Delta G(T)$ is given by Eq. 5 and $f(D,T)$ describes the urea dependence of the free energy. Two models have been considered to treat the urea dependence of the free energy function. The linear model (35–37) imposes a linear dependence on urea concentration (D), where the m value is affected by temperature in a manner similar to the free energy of unfolding and takes the expression in brackets in Eq. 8:

$$f(D, T) = \left[\Delta H_g (1 - (T/T_g)) - \Delta C_{P,g} ((T_g - T) + T \, ln(T/T_g))\right] \times D. \quad (8)$$

On the other hand, the preferential binding model (38,39) attributes the urea unfolding of the protein to preferential binding to the unfolded state and, for independent and similar urea binding sites, provides the following expression for $f(D,T)$:

$$f(D, T) = \Delta n RT \ln\left(1 + D e^{-\Delta G_b(T)/RT}\right), \quad (9)$$

where Δn is the difference in the number of urea binding sites between the unfolded and native states, and $\Delta G_b(T)$ is the free energy of binding, given by

$$\Delta G_b(T) = \Delta H_b - T\Delta S_b + \Delta C_{P,b} \times (T - 298.15 - T \ln(T/298.15)), \quad (10)$$

where ΔH_b, ΔS_b, and $\Delta C_{P,b}$ are the enthalpy, entropy, and heat capacity changes of binding at 298.15 K, respectively.

Spectra deconvolution and analysis of conformation stability as a function of pH

The populations of native state and molten globule at 25°C, in the absence of denaturant, and at different pH values (1.8, 2.0, 2.2, 2.4, 2.5, 2.75, 3.1, 3.7, 4.1, and 5.0), were calculated by deconvolution of far-UV CD spectra, using

$$Y(pH) = Y_N X_N(pH) + Y_{MG} X_{MG}(pH), \quad (11)$$

where $X_{MG}(pH) = 1 - X_N(pH)$ and the spectra of native and molten globule states are known (spectra at pH 1.8 and 5.0). To calculate the free energy difference between the two states (ΔG_{N-MG}) in the absence of denaturant and at the different pH values, the calculated populations of the native state at different pH values were introduced into Eq. 12:

$$X_N = \frac{1}{1 + e^{-\Delta G_{N-MG}/RT}}. \quad (12)$$

The different ΔG_{N-MG} values so obtained make it possible, using Eq. 13, to evaluate the number of protons that drive the native/molten globule transition and their pK_a values in the two conformations:

$$\Delta G_{N-MG} = \Delta G^0_{N-MG} - n_1 RT \ln\left(\frac{1 + 10^{pK_a^{MG} - pH}}{1 + 10^{pK_a^{N} - pH}}\right), \quad (13)$$

where ΔG^0_{N-MG} represents the pH-independent difference in stability when the protein is completely unprotonated, n_1 is the number of residues in the native conformation whose pK_a in the molten globule is different enough to modify the proton content in the states, and pK_a^{MG} and pK_a^{N} are their mean pK_a values in those states.

Once the populations of the molten globule and native states in the pH 1.5–5 interval are known, their stabilities relative to the unfolded conformation have been determined from urea unfolding curves at different pHs that have been globally fitted to a three-state model in the pH transition region (pH values 2.2, 2.6, and 3.2), and to a two-state model at pH 1.6 and 2.0 (molten globule/unfolded) and pH 3.9, 4.4, and 5.0 (native/unfolded). The stabilities of the molten globule (ΔG_{MG-U}) make it possible to determine the number of residues, n_2, in the molten globule whose pK_a in the unfolded state is sufficiently different to modify the proton content in the states and the mean pK_a values in those states, pK_a^{MG} and pK_a^{U}, using Eq. 14.

$$\Delta G_{MG-U} = \Delta G^0_{MG-U} - n_2 RT \ln\left(\frac{1 + 10^{pK_a^U - pH}}{1 + 10^{pK_a^{MG} - pH}}\right). \quad (14)$$

Estimation of protein stabilization by dextran using equivalent scaled particle theory

According to the scaled particle theory (40,41), the difference in free energy between two conformations of a given protein (herein the native and molten globule states of apoflavodoxin: ΔG_{MG-N}) is influenced by excluded volume effects exerted by crowding agents (herein dextran) according to

$$\Delta G_{MG-N} = \Delta G^0_{MG-N} - (B_{MG/dex} - B_{N/dex})RT[\text{dextran}], \quad (15)$$

where ΔG^0_{MG-N} is the free energy difference in absence of crowding agent, $B_{MG(N)/dex}$ is an interaction coefficient between protein and polymer (constant for a given protein conformation and polymer under a fixed set of solution conditions), and the concentration of polymer is given in weight/volume units. Equation 15 can be written as

$$\Delta G_{MG-N} = \Delta G^0_{MG-N} - m_{MG-N}[\text{dextran}], \quad (16)$$

where the value of $m_{MG\text{-}N}$ can be estimated using the excluded volume model of Ogston (42) as

$$m_{MG-N} = \left[(1 + r_{MG}/r_{dex})^2 - (1 + r_N/r_{dex})^2\right]\upsilon_{dex}RT, \quad (17)$$

where r_{MG} and r_N are the effective sphere radii of the molten globule and native states of the protein, r_{dex} is the effective cylindrical radius of dextran, and υ_{dex} is the effective specific excluded volume of dextran. For *H. pylori* apoflavodoxin stabilization by dextran at pH 2.5, m_{MG-N} was calculated from $r_{dex} = 7$ Å (43), $\upsilon_{dex} = 0.0008$ L g^{-1} (44), $r_N = 18.8$ Å, $r_{MG} = 20.6$ Å, and $r_U = 39.0$ Å (25).

FMN binding to apoflavodoxin

The thermodynamic parameters of the interaction between molten globule apoflavodoxin and its FMN cofactor were determined in 23 mM phosphate buffer pH 2.0 at 25°C by fluorescence spectroscopy and isothermal titration calorimetry (ITC) (VP-ITC calorimeter, Microcal LLC, Northampton, MA). The FMN used in both ITC and spectroscopic determinations was supplied by Sigma-Aldrich (>95% pure). In the ITC experiments, a 10-μM flavodoxin solution was loaded in the calorimetric cell and titrated with 90 μM FMN dissolved in the same buffer. Both solutions had been previously degassed. Between injections, it took 400 s to recover the baseline. On the other hand, the quenching of flavin fluorescence at 525 nm upon addition of small aliquots of apoflavodoxin was recorded and the following equation was used to fit the fluorescence data:

$$F = F_f + \frac{F_b - F_f}{2C_L}\left[C_P + C_L + K_d - \sqrt{(C_P + C_L + K_d)^2 - 4C_P C_L}\right], \quad (18)$$

where F_f and F_b are the fluorescence signals of free and bound ligand, respectively; C_L is the total ligand concentration; C_P is the total protein concentration; and K_d is the dissociation constant.

RESULTS AND DISCUSSION

Stability of the molten globule state at pH 2.0

At low pH, *H. pylori* flavodoxin populates a molten globule conformation that is compact, rich in secondary structure, and devoid of, or perhaps exhibiting very weakened, tertiary native interactions, and which displays exposed hydrophobic patches where the fluorescent probe ANS can bind (25). It is slightly expanded relative to the native state (30% volume increase) and remains monomeric at pH 2.0 (25), unlike the molten globule previously found at acidic pH for the homologous *Anabaena* apoflavodoxin. *H. pylori* apoflavodoxin molten globule thus constitutes a fine model to investigate the energetics of this kind of conformation, which have been implicated in the mechanism of protein folding (10,11) and a variety of physiological processes, such as protein membrane translocation (12,13) or enzyme inactivation (13,45), or as constituents of substrates of chaperonins (46). It has also been proposed that they participate in the mechanism of amyloid fibril formation (47). On the other hand, it has become increasingly clear that, in native conditions, the native state of many proteins is accompanied by a cohort of partly unfolded conformations of low population but close in energy and ready to become dominant under a variety of stress conditions (2). Whether molten globules belong to the native ensemble remains to be determined. Here, we have investigated the conformational stability of *H. pylori* apoflavodoxin molten globule and its relationship to the native state ensemble, which for flavodoxins includes up to two partly unfolded conformations that become dominant upon heating (6,24) and, for one of them, upon mutation (29,30). Stability has been first studied at pH 2.0 using urea-induced and thermally induced unfolding. Both chemical and thermal unfolding are reversible, as is shown by the fact that the unfolding curves obtained from refolded protein samples are very similar to those obtained from fresh samples (same thermodynamic parameters with a signal lost of ~10%, not shown). In addition, no protein concentration dependence was noticed (from 2 μM to 20 μM), which indicates that the unfolding is free from complicating oligomerization or aggregation processes. For urea-induced unfolding, fluorescence and far-UV CD curves are superimposable (Fig. 1 *A*) and have been globally fitted to a two-state model (Eq. 2). The stability of the molten globule is very low (1.13 ± 0.05 kcal/mol; mean of three experiments ± SE); and the *m* value of 1.33 ± 0.043 kcal/(mol × M), well below the *m* value of 2.32 ± 0.02 kcal/(mol × M) described for the native con-

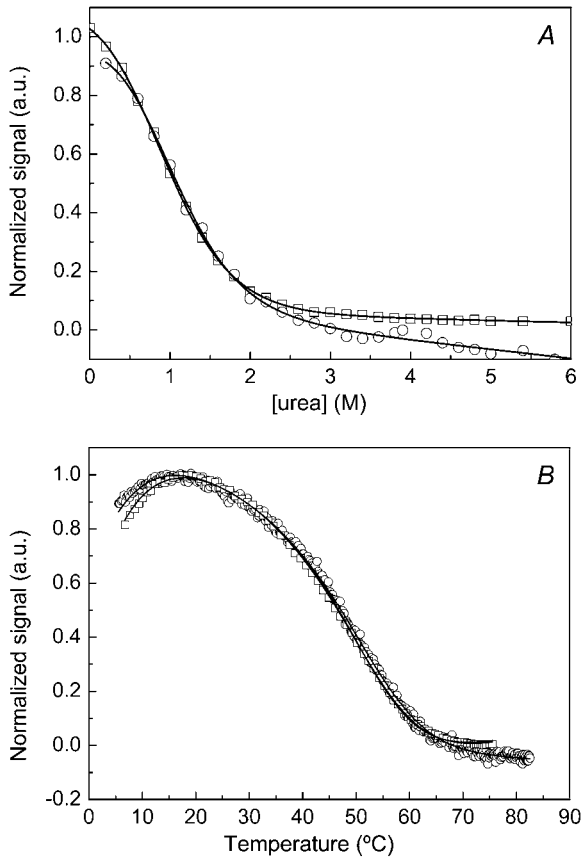

FIGURE 1 Apoflavodoxin unfolding at pH 2.0. (*A*) Urea-induced unfolding and (*B*) thermally induced unfolding of the molten globule state of apoflavodoxin followed with fluorescence (*squares*) and far-UV CD (*circles*). For a better visual comparison, data were normalized so that the signals are from roughly 0 to 1. The lines represent the global fit to a two-state unfolding model.

formation at pH 5 (25), is consistent with the molten globule being more hydrated than the native state.

Fluorescence and far-UV CD thermal unfolding curves (Fig. 1 *B*) can also be superimposed and have also been globally fitted to a two-state model (Eq. 4). The molten globule thus exhibits a much simpler thermal unfolding behavior than the native conformation, which unfolds via a four-state equilibrium (24). The temperature of mid-denaturation (49.6 ± 0.5°C; mean of three global fits ± SE) is not particularly low, and it lies between the values of $T_{m1} = 31.9$ and $T_{m2} = 57.9$°C described for the native conformation at pH 9.0 (24). The enthalpy change (25 ± 1 kcal/mol) is nevertheless much lower than that of the native state at pH 9.0 at the same temperature (~85 kcal/mol at 49.9°C), which is expected for a conformation with debilitated tertiary interactions. The thermal unfolding has not been studied by differential scanning calorimetry because, due to the low enthalpy change, the protein concentration required is high and leads to protein precipitation at high temperatures (unlike in the low protein concentration range used for spectroscopic thermal unfolding). This phenomenon, observed at high protein concentrations and high temperatures, seems to be preceded by conversion into a conformation of high beta content (not shown).

To extrapolate the stability data to lower temperatures and compare thermal and chemical unfolding, the ΔC_P value is required. Often, ΔC_P values derived from spectroscopic thermal unfolding curves are completely unreliable (48). However, when cold denaturation is observed within the experimental temperature window, the ΔC_P values so obtained are reasonable, because cold denaturation is strongly linked to ΔC_P. As shown in Fig. 1 *B*, cold denaturation of the molten globule is clear and the ΔC_P value derived from the global fit of the thermal unfolding curves (1.1 ± 0.2 kcal/(mol × K); mean of three determinations ± SE) should be a good approximation. Nevertheless, to obtain a more precise ΔC_P value, thermal unfolding of the molten globule has been carried out in the presence of different urea concentrations, which induces a more pronounced cold denaturation in the experimental temperature window (Fig. 2). At 1.4 M urea, the unfolding curve is almost symmetrical, showing two clear transitions, one corresponding to heat denaturation and the

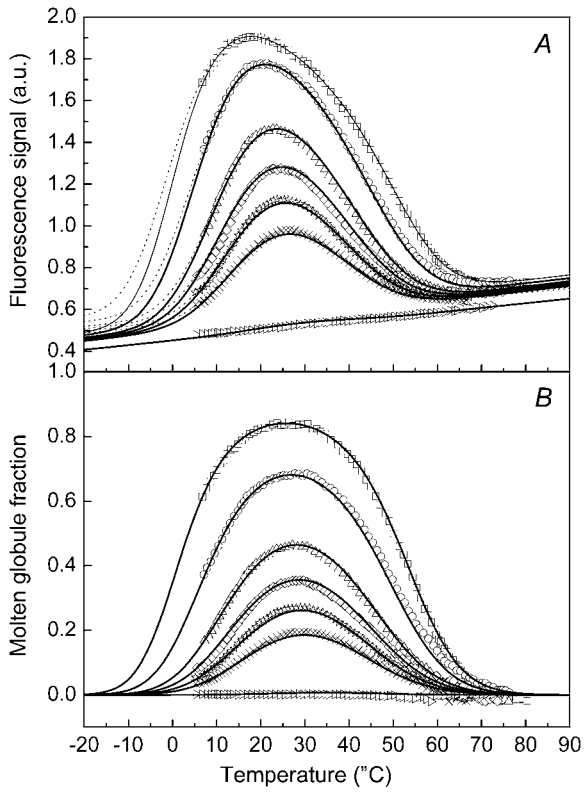

FIGURE 2 Cold denaturation in apoflavodoxin. (*A*) Thermal unfolding curves of apoflavodoxin at pH 2.0 in the absence of urea (*squares*) and in the presence of 0.4 (*circles*), 0.8 (*triangles*), 1 (*rhombus*), 1.2 (*stars*), 1.4 (*crosses*), and 3 M (*open arrowheads*) urea. All curves were globally fitted to the two-state model for thermal unfolding coupled to either the linear extrapolation method (*solid lines*) or the urea-binding method (*dotted lines*) for chemical unfolding. (*B*) The molar fraction of the molten globule state obtained for each experimental curve and its theoretical value calculated using the parameters obtained for the two-state unfolding model coupled with the linear extrapolation model for the interpretation of urea influence (*solid lines*).

other, at low temperatures, to cold denaturation. At 3 M urea, the protein is completely unfolded, which is consistent with the urea unfolding curve in Fig. 1 *A*, and no thermal transition is observed. The smooth linear temperature dependence of the fluorescence of the denatured state at 3 M urea from 0 to 85°C (at 320 nm—not shown, but see Fig. 2 *A* for the ratio of emissions at 320 and 360 nm) suggests that the cold- and heat-denatured states may exhibit a similar degree of compaction. Global fits of the curves to either the linear model (35–37) or the urea binding model (38,39) are good (Fig. 2 *A*), the global fitting error being slightly lower for the linear model. The two models yield similar values for the thermodynamic parameters of molten globule thermal unfolding in the absence of denaturant ($T_m = 50.4 \pm 0.3$ or 47.9 ± 0.7°C, $\Delta H_m = 26.8 \pm 0.8$ or 23 ± 1 kcal/mol, $\Delta C_P = 1.09 \pm 0.02$ or 0.98 ± 0.03 kcal/(mol × K) for the linear and urea-binding models, respectively) (Fig. 2 *A*). At 25°C, the linear model provides an *m* value of 1.36 kcal/(mol × M), in excellent agreement with the value obtained from simple urea unfolding curves: 1.33 ± 0.04 kcal/(mol × M) (Fig. 1 *A*). The urea-binding model estimates that ~143 ± 40 urea molecules bind preferentially to the unfolded state relative to the molten globule, with a binding enthalpy of -1.76 ± 0.09 kcal/mol and a binding entropy of -0.014 ± 0.005 kcal/(mol × K) per urea molecule, in good agreement with the values proposed by Makhatadze and Privalov (-2.1 ± 0.5 kcal/mol and -0.013 ± 0.002 kcal/(mol × K), respectively) for urea unfolding of native proteins (39). Therefore, preferential binding of urea to the unfolded state leads to significant decreases of the apparent enthalpy and entropy of unfolding, which makes cold denaturation take place at higher temperatures. On the other hand, the heat capacity change of urea binding to the protein is calculated at 0.04 ± 0.001 kcal/(mol × K), which means that urea increases the curvature of the stability curve (49), thus further raising the temperature of cold denaturation of the molten globule. From the thermodynamic values calculated using the linear model (see Table 4), the conformational stability of the molten globule at 25°C in the absence of denaturant is of 0.99 ± 0.07 kcal/mol, in good agreement with the value derived from chemical denaturation analysis (1.13 ± 0.05 kcal/mol). Overall, the thermal and chemical stability data consistently indicate that at 25°C and pH 2.0, 85% of the apoflavodoxin molecules are in the molten globule conformation and 15% are cold-denatured.

It has been reported that ΔC_P and *m* values of protein unfolding are correlated to protein size (32,50). Apoflavodoxin from *H. pylori* contains 164 residues. The ΔC_P of the native state at pH 9 (calculated, as described by Cremades et al. (24), to be 2.7 kcal/(mol × M)) is consistent with a protein of ~147 residues, whereas the ΔC_P of the molten globule at pH 2.0 corresponds to that of a native protein of 70 residues. It thus seems that the molten globule is hydrated so that about half of the residues behave as if they where exposed to solvent as much as in the denatured state. Exactly the same picture is provided by the *m* values, which predict a length of 182 residues for the native state but only 96 for the molten globule (32,50).

The native-molten globule transition

At pH 5.0, the native conformation of *H. pylori* apoflavodoxin, of known x-ray structure (21) and well characterized thermodynamic behavior (24,25), is largely dominant. However, as the pH drops, the stability balance between native state and molten globule switches, so that at pH 2.0 most folded protein molecules are molten globules. At intermediate pH, different populations of both states are expected. To determine the free energy difference of the molten globule/native equilibrium and the influence of pH therein, a careful spectroscopic and thermodynamic global analysis has been performed combining data from the pH range 1.5–5.0. First, native and molten globule molar fractions at the different pHs in the transition region have been calculated from deconvolution of apoflavodoxin spectra recorded at different pH values from 1.5 to 5. Deconvolution was based on far-UV CD spectra (Fig. 3 *A*, *inset*). Fluorescence and near-UV CD

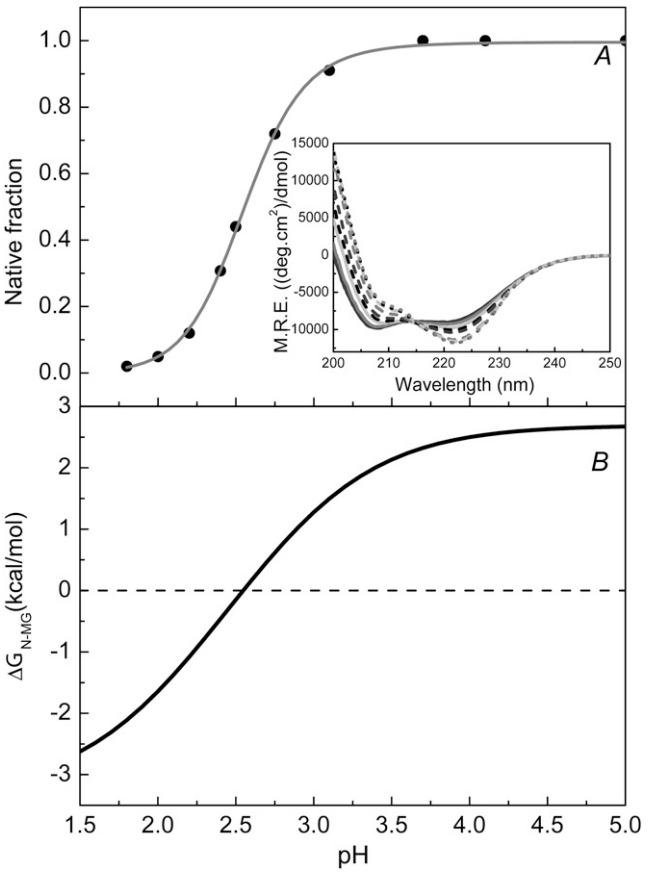

FIGURE 3 The native/molten globule equilibrium as a function of pH. (*A*) Native state molar fraction obtained at 10 different pH values from 1.8 to 5 from deconvolution of far-UV CD spectra (*inset*). Solid lines represent the fit of the data to Eq. 12. (*B*) pH dependence of the free energy difference between native and molten globule states obtained from fitting native fraction data to Eqs. 12 and 13.

spectra were not used due to strong influence of protonation in fluorescence emission intensities and weak near-UV CD spectra, respectively. The native fraction as a function of pH is shown in Fig. 3 *A* and the free energy difference between native and molten globule in Fig. 3 *B*. The transition from native state to molten globule is driven by preferential proton binding to the molten globule of around five acidic residues of the protein, the pK_as of which are higher in the molten globule (2.9) than in the native state (2.0). The reason for increased pK_as in the molten globule can be either that the affected residues are more buried in the molten globule than in the native state, which seems unlikely, or that they establish specific interactions that stabilize the ionized forms in the native state, but are broken in the molten globule conformation. As the pH drops, the increase in proton concentration promotes a preferential stabilization of the molten globule, which is more easily protonated than the native state. A tentative identification of the acidic residues involved in the native/molten globule transition has been made by calculating the pK_as of all apoflavodoxin ionizable residues in the native structure (21) using the program PROPKA (51). Six candidate residues are Asp-33, Asp-63, Asp-75, Asp-88, Glu-98, and Asp-140, the pK_as of which are calculated to be $<$3.1. These residues appear to be spread on the protein surface (not shown). Therefore, if the prediction is correct, the *H. pylori* apoflavodoxin molten globule could be a homogenously destabilized conformation, as has been described for a molten-globule-like shortened version of *Anabaena* apoflavodoxin, whose low-resolution structure was solved by equilibrium Φ-analysis (8). On the other hand some of these residues are located at or near the FMN binding site, which suggests that this site could be severely distorted in the molten globule. Two contrasting structural models have been proposed for molten globules: expanded conformations with locally stable native secondary-structure subdomains that are partially folded but permit water penetration (52), or conformations with a dry, native-like hydrophobic core plus an unfolded surface (53). Either model can explain both the increased volume and the low heat capacity and *m* values of the apoflavodoxin molten globule. However, its close-to-native helical content argues in favor of the first model, because the helices of its α/β fold are located at the surface (21).

The stabilities of the native and molten globule states relative to the unfolded one have also been determined, as explained in the Methods section. The global fit to the three-state model at pH values with significant molar fraction of the three species (pH 2.2, 2.6, and 3.2) is good (Fig. 4 *A*). The populations of each state at these intermediate pH values are shown in Fig. 4, *B–D*. The overall stability of the protein ($\Delta G_{N-U} = \Delta G_{N-MG} + \Delta G_{MG-U}$) at different pHs was fitted to Eq. 13 plus Eq. 14, and from this fit, the number of molten globule residues involved in its pH-induced unfolding transition has been determined (Table 1). Molten globule unfolding is driven by preferential binding of protons to the denatured state. Three side chains whose pK_as are lower in the molten globule (2.9) than in the unfolded state (3.9) are involved. These groups are most likely carboxylates, but the lack of a structural model for the molten globule precludes any tentative assignment. That the mechanism driving molten globule unfolding at low pH is the same one that promotes conversion of the native state into the molten globule highlights the fact that the differences between native protein conformations and molten globules are in many respects of a quantitative rather than qualitative nature (27).

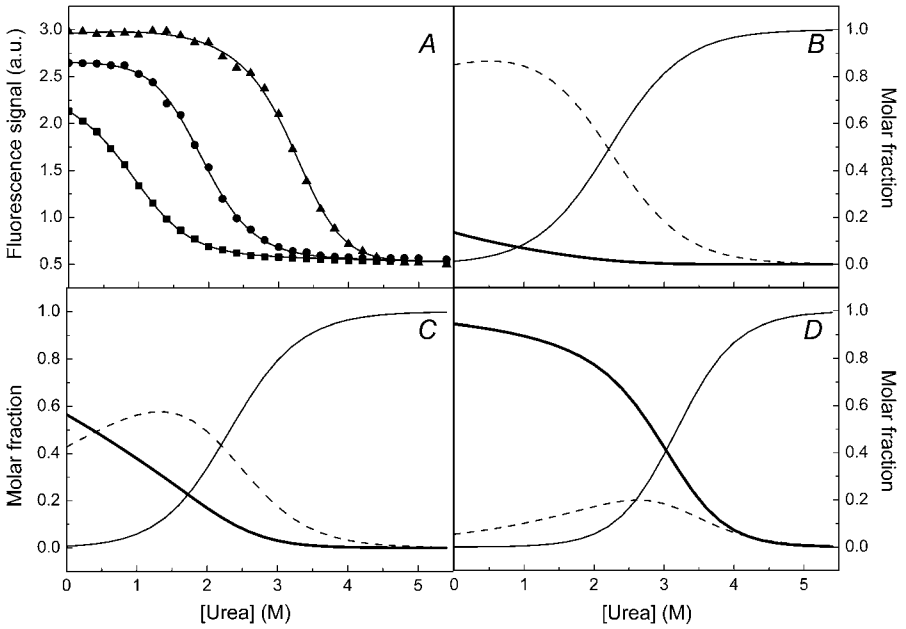

FIGURE 4 Three-state apoflavodoxin urea unfolding at pH values where native, molten globule, and unfolded states are significantly populated. (*A*) Global fit of urea-unfolding curves at pH 2.2, 2.6, and 3.2 to a three-state unfolding model (Eq. 3). (*B–D*) Calculated populations as a function of urea concentration of native (*thick solid lines*), molten globule (*dashed lines*), and unfolded states (*thin solid lines*) at pH 2.2, 2.6, and 3.2, respectively.

TABLE 1 Parameters defining the conformational stability of native and molten globule *H. pylori* apoflavodoxin as a function of pH (N ⇄ MG ⇄ U)

n_1	pK_a^N	pK_a^{MG}	ΔG^0_{N-MG}	n_2	pK_a^U	ΔG^0_{MG-U}
4.9 ± 0.6	2.0 ± 0.3	2.9 ± 0.1	2.7 ± 0.32	2.8 ± 0.2	3.9*	6.4 ± 0.2

Free energies are given in kcal/mol. Fitting errors are reported. Temperature and ionic strength are 25°C and 10 mM, respectively.
*The pK_a^U value was fixed during the fitting to reduce dependency between parameters. It represents a weighted average of the expected pK_as of aspartic and glutamic residues in unfolded *H. pylori* flavodoxin.

Can molecular crowding stabilize native proteins relative to partly unfolded intermediates? Effects of crowding agents on molten globule stability and on native/molten globule state equilibrium

Macromolecular crowding has been shown to stabilize compact forms of proteins (41,54,55). According to excluded volume theory (55), crowding agents provide a nonspecific force that promotes a reduction of total excluded volume, leading to stabilization of the most compact conformations of proteins. Therefore, the higher the volume difference between conformations, the greater the stabilizing effect. According to the scaled-particle theory (56–58), the free energy difference between two protein conformations depends linearly on crowding agent concentration. For the molten globule/native state equilibrium in *H. pylori* apoflavodoxin, the *m* parameter in Eqs. 16 and 17 is expected to be 0.00093 (kcal × L)/(mol × g), much lower than the value of 0.0156 (kcal × L)/(mol × g) calculated for the unfolded/native equilibrium. With those *m* values, a 1 kcal/mol stabilization of the native state relative to the molten globule would require 1000 g/L dextran in the media, whereas for global unfolding of the native protein, such stabilization would be achieved with only 50 g/L.

To test the performance of the theory and to investigate whether crowding can induce a significant stabilization of native proteins relative to equilibrium intermediates close in energy, the effect of dextran on the stability of *H. pylori* apoflavodoxin was tested in several pH conditions that favor either the molten globule or the native state, and also at a pH value where the two conformations display the same molar fraction (pH 2.55). At this pH value, different dextran concentrations from 0 to 250 g/L were used, and spectroscopic properties (fluorescence emission maximum wavelength and mean residue ellipticity at 222 and 208 nm) were carefully monitored to try to sense slight variations in native and molten globule populations (Fig. 5 *A*). Within the 0–250 g/L dextran concentration range, the wavelength of maximal emission remains constant at 328.5 nm, compared to 323.5 nm for the native conformation at pH 5.0, and the ellipticity similarly remained constant. Therefore, 250 g/L dextran seems unable to significantly shift the conformational equilibrium toward the native state.

On the other hand, the influence of 100 g/L dextran on the conformational stability of the molten globule at pH 2.0 and

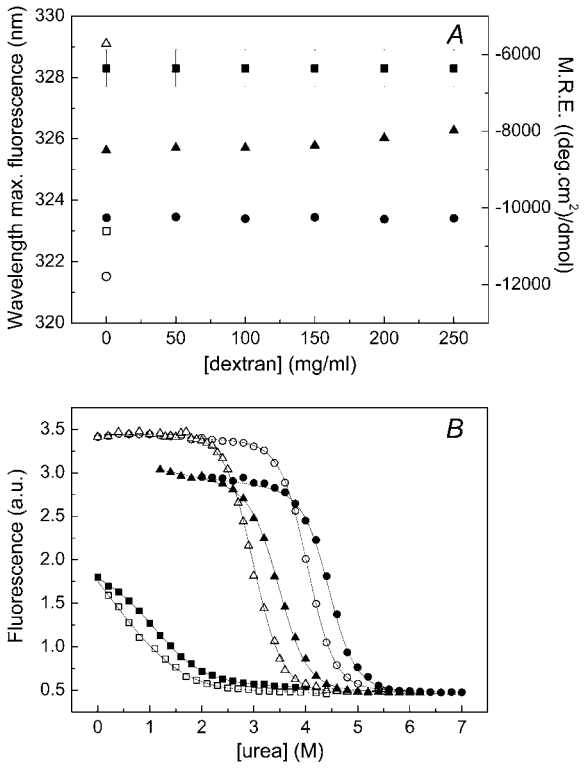

FIGURE 5 Stabilization of native and molten globule apoflavodoxin by dextran. (*A*) Spectroscopic signals of apoflavodoxin at pH 2.55 (50% of the protein in the native state and the other 50% in molten globule conformation) at different concentrations of dextran (*solid symbols*): the wavelength of the maximum in fluorescence emission intensity (*squares*) and the CD signal at 222 nm (*circles*) and 208 nm (*triangles*). For comparison, the signals of the protein at pH 5 (100% of the protein in the native state) are also shown as open symbols. (*B*) Urea-unfolding curves of apoflavodoxin in the absence (*open symbols*) and presence (*solid symbols*) of 100 mg/mL of dextran, assessed by fluorescence emission at pH 2 (*squares*), pH 5 (*circles*), and pH 7 (*triangles*). Black lines are individual fits of the data to Eq. 2.

of the native state at pH 5.0 and 7.0 was determined by urea denaturation (Fig. 5 *B*) and compared with the predictions from the scaled-particle theory (Table 2) together with the excluded volume theory by Ogston (42). Since both molten globule and native state experience large volume increases when they unfold (25), theory predicts significant and similar stabilizations at ~1.5–1.6 kcal/mol. Indeed, similar stabilization of 0.8–0.9 kcal/mol (see Table 2) was observed for the native state at pH 5 and 7, and the molten globule at pH 2 is also significantly stabilized by ~0.5 kcal/mol. The lack of perfect agreement between the lower observed stabilizations and theory predictions may be attributed to various things, including inaccuracy of the value of the radius of the unfolded conformation introduced in Eq. 17 and the possibility that the unfolded state at low pH is more compact than at higher pH values. Whatever the reason, it seems clear that the two compact conformations analyzed here (the native state and the molten globule) are notably stabilized by crowding effects against full unfolding. In a similar way, strong stabilization of a homologous flavodoxin by crowding agents

TABLE 2 Stabilization of apoflavodoxin in macromolecular crowding conditions

		Without dextran*		100 mg/mL dextran		Stabilization	
Transition	pH	m	ΔG_w	m	ΔG_w	Determined	Predicted†
MG⇄U	2	1.35 ± 0.04	1.13 ± 0.05	1.30 ± 0.03	1.59 ± 0.05	0.5 ± 0.1	1.5
N ⇄ U	5	2.32 ± 0.02	9.37 ± 0.08	2.25 ± 0.10	10.28 ± 0.51	0.9 ± 0.5	1.6
N⇄U	7	2.18 ± 0.06	6.56 ± 0.2	2.09 ± 0.08	7.38 ± 0.35	0.8 ± 0.4	1.6
N ⇄ MG	2.55					Not detected	0.1

Protein stability was determined by urea-induced unfolding followed by fluorescence emission at 25°C in 23 mM sodium phosphate, pH 2.0, 16 mM sodium acetate, pH 5.0, and 30 mM MOPS, pH 7.0. m values are given in kcal/(mol × M), and ΔG_w and stabilization values in kcal/mol. Reported errors are experimental errors.

*Data for apoflavodoxin without dextran are taken from Cremades et al. (25).

†Stabilization of apoflavodoxin in the presence of 100 mg/mL dextran were predicted by scaled particle theory (Eqs. 16 and 17).

has been described recently (59) using analysis of circular dichroism thermal unfolding curves, which in flavodoxins typically monitor the conversion of a compact intermediate into the fully unfolded state (59) and therefore report on a conformational transition of large volume change. In contrast, we have shown here that, according to our spectroscopic analysis and also according to theory predictions, the relative stability of the native and molten globule states in solution conditions where they coexist (pH 2.55) does not appear to be modified by crowding agents. This is an important issue, because many proteins are transformed, under a variety of stress conditions, into partially unfolded conformations (such as molten globules (27), thermal equilibrium intermediates (6,24), or partly unfolded mutants (29,30)) rather than the unfolded state. It should be borne in mind that for proteins experiencing non-two-state equilibrium unfolding, it is useful to distinguish between the relevant stability associated with the N↔I equilibrium and the residual stability of the intermediate conformation (I↔U), the two stabilities that add up to the global stability of the protein (N↔U) (60,61). According to scaled-particle theory and to the observations reported here, such proteins, which may well be a majority within the proteome, will not benefit from crowding as a stabilizing force, because the volume changes involved in the N↔I transitions will not be large in many cases.

Can osmolytes drive molten globules into native conformations?

A variety of organisms use protein-stabilizing osmolytes, such as trimethylamine N-oxide and the disaccharides α, α-trehalose and sucrose (62), to survive at extreme temperatures, in dehydration, and under other stress conditions (63–66). Proteins are more stable in the presence of osmolytes, because osmolytes preferentially increase the Gibbs energy of the protein denatured state (67–71), likely due to unfavorable interactions between polypeptide backbone and osmolyte (the so called ''osmophobic effect'' (69)). Examples of mechanisms proposed to account for this preferential exclusion include solvophobicity (69,72), surface tension (73–75), excluded volume (76,77), water structure changes, and electrostatic repulsions (68). Recently, the effect of sugars on the conformation of several unfolded proteins has been studied and it has been proposed that volume exclusion by high concentrations of sugars can induce a compact molten globule conformation from the acidic unfolded state of some proteins (78,79). In this study, we tested whether osmolytes can similarly induce the transformation of molten globules into native structures. We first tried trimethylamine N-oxide (63,80,81), but it makes the molten globule aggregate, as do several other salts we have tested (not shown), which prompted us to use a neutral osmolyte such as sucrose. Shifts in the native/molten globule equilibrium at pH 2.55 (where they are present in equimolecular concentrations) were investigated in 20 μM apoflavodoxin solutions by recording the CD signal at 222 nm as a function of sucrose concentration (from 0 to 1.5 M). Although the helical content increases at high sucrose concentrations approaching that of the native state, the expected concomitant decrease of the minimum at 208 nm (25) (Fig. 3 *A*, *inset*) does not take place (not shown). On the other hand, the wavelength of maximal tryptophan fluorescence emission moves to lower values at high sucrose concentrations, suggesting a lower exposure to solvent of the tryptophan residues. Nevertheless, the same effect is observed at pH 5.0, where the native conformation is prevalent (not shown). It seems thus that sucrose increases both molten globule and native state compactness without driving the molten molecules into the native conformation. The reason this osmolyte can drive conversion of unfolded proteins into molten globules (78,79) but fail to drive conversion of molten globules into native proteins (this work) may also be related to the volume differences between native proteins and molten globules being smaller than those between molten globules and unfolded states.

Osmotic stress analysis (82) is sometimes used to determine hydration changes from osmolyte-induced changes in equilibrium constants. Our data could be interpreted, within the framework of osmotic stress analysis, as indicating that molten globule and native apoflavodoxin are similarly hydrated, which seems unlikely considering their very different m-values of urea unfolding.

Native state rescue by the FMN cofactor

Preferential ligand binding to a specific protein conformation stabilizes that conformation relative to alternative conformations (83–86). To determine whether FMN, the natural flavodoxin cofactor, can bind to the apoprotein in acidic conditions and rescue the native state, FMN was added at different concentrations to a 20 μM apoflavodoxin solution at pH 2.55. An equimolar 20-μM concentration of FMN was enough to recover the native wavelength of maximal fluorescence emission and the native CD signals at both 222 and 208 nm, which became almost identical to those exhibited by holoflavodoxin at pH 5 (not shown). FMN can therefore bind to the native state at acidic pH, thus shifting the molten globule/native state equilibrium toward the native conformation.

The affinity of the apoflavodoxin:FMN complex was then determined at pH 2.0, where all the protein is in the molten globule conformation, by both fluorescence quenching of FMN upon apoprotein binding and by ITC (Fig. 6, *A* and *B*, respectively), and the corresponding binding parameters, essentially identical for the two techniques, are reported in Table 3. Compared to the functional complex at pH 7.0 (24), the apparent affinity is 100 times lower, whereas the enthalpy and entropy of binding are much higher (Table 3). It should be noted, however, that these are not the true binding parameters to native apoflavodoxin because part of the binding energy of the complex is utilized to shift the molten globule/native equilibrium toward the binding-competent native state. The binding energy was therefore corrected by adding up the previously determined free energy difference between native state and molten globule at pH 2.0. As regards the enthalpy and entropy of binding, they are not expected to change significantly with pH. First, FMN binding at pH 7.0 and 9.0 has been reported to take place without proton exchange (24), and second, very similar binding free energies are obtained at pH 2.0 (Table 3, *corrected value*), 7.0, and 9.0 (24). Therefore, we propose that the intrinsic entropy and enthalpy of binding at pH 2.0 are similar to those at pH 7, and that the differences between these values and the apparent values experimentally determined by titration of the molten globule with FMN provide estimations of the enthalpy and entropy contributions (−23.6 and 25.7 kcal/mol, respectively) associated with the conversion of the molten globule to the native state at pH 2.0 and 25°C. According to this interpretation, adding up the enthalpic and entropic contributions, the conformational stability of molten globule apoflavodoxin at pH 2.0 relative to the native state is calculated at 2.1 kcal/mol, which agrees well with the value directly determined from deconvolution analysis of far-UV CD spectra ($\Delta G_{MG-N} = 1.64$ kcal/mol, Fig. 3 *B*). The relatively high value of the enthalpy change from the molten globule to the native state (yet only one-half of the unfolded/native enthalpy change at pH 9.0 at 25°C (24)) suggests that many internal interactions are formed or strengthened during the conformational change, whereas the unfavorable entropic contribution indicates that ordering of the polypeptide chain offsets the expected increase in solvent entropy.

The equimolecular mixture of apoflavodoxin and FMN at pH 2.0 and 25°C presents spectroscopic properties similar to those at pH 5.0, 7.0, and 9.0 (24) (Fig. 7). This spectral coincidence indicates that there is a single holoflavodoxin conformation in the 2.0–9.0 pH interval. The stability of holoflavodoxin at pH 2.0 has been studied by monitoring thermal unfolding curves with different spectroscopic techniques (Fig. 8 *A*). The unfolding is reversible provided the temperature is kept below 62°C; otherwise, the released FMN group hydrolyzes and the apoprotein refolds but cannot

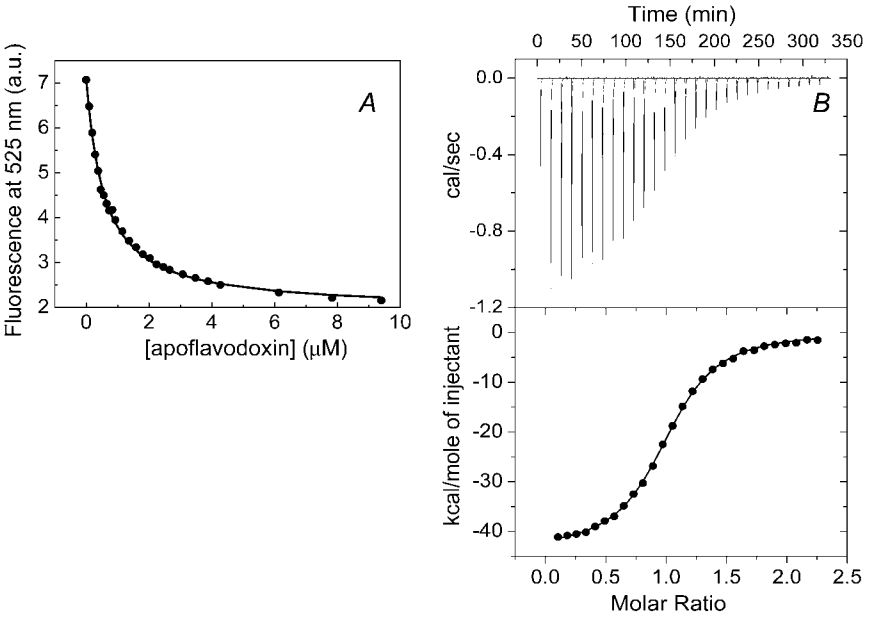

FIGURE 6 Rescue of native apoflavodoxin at pH 2.0 by FMN binding. (*A*) FMN fluorescence quenching upon apoflavodoxin binding and (*B*) isothermal titration calorimetry were used to measure the affinity constant of the flavodoxin/FMN complex at pH 2.0 and to estimate the thermodynamic parameters of binding.

TABLE 3 Thermodynamic parameters of FMN binding to flavodoxin at pH 2.0 at $T = 25°C$

Technique	K_d (μM)	ΔG_b (kcal/mol)	ΔH_b (kcal/mol)	$-T\Delta S_b$ (kcal/mol)
Spectroscopy	0.53 ± 0.04	−8.6 ± 0.2	–	–
ITC	0.40 ± 0.01	−8.7 ± 0.1	−43.6 ± 0.2	34.9
Corrected values*	–	−10.37†	−20‡	9.2‡

*Binding parameters obtained from the experiments have been corrected to take into account that part of the binding energy is required to shift the conformational equilibrium toward the native state (see text). These corrected values are the real binding parameters of FMN to the apoflavodoxin native state.

†Free energy change was calculated by adding the energy difference between the native and molten globule states at pH 2 to the apparent binding energy.

‡These values correspond to binding parameters determined at pH 7 (24) (see text for a detailed justification). In particular, they are consistent with the experimentally determined free energy difference of the MG↔N equilibrium.

bind FMN (not shown). The different unfolding curves are not superimposable (Fig. 8 *A*), which demonstrates the appearance of an equilibrium intermediate. The intermediate has lost the near-UV CD signal characteristic of the associated FMN cofactor and accumulates at temperatures where the molten globule conformation of the apoprotein is still stable (Fig. 8 *B*). That the intermediate corresponds to the molten globule is also shown by the thermodynamic parameters obtained from global three-state analysis of the four holoflavodoxin unfolding curves at pH 2.0 (Table 4). Indeed, the second transition takes place at a temperature and with an enthalpy change nearly identical to those determined for molten globule thermal unfolding (49.6 ± 0.5°C and 25 ± 1 kcal/mol). The thermal unfolding of holoflavodoxin at pH 2.0 can thus be described by the scheme

$$\text{Holo} \rightleftarrows \text{MG} \rightleftarrows \text{U}$$

As already discussed, ΔC_P values obtained from spectroscopic unfolding curves should be observed with caution. In this particular case, however, ΔC_{P2} can be identified with the value accurately determined for molten globule unfolding (Fig. 2), whereas the value obtained for ΔC_{P1} is reasonable because, added to ΔC_{P2}, it amounts to 2.6 kcal/(mol × K), which compares well with the overall heat capacity change of 2.7 determined for the protein (24). The stability of the three conformations and their relative populations can thus be calculated as a function of temperature (Fig. 8 *B*). As can be seen, FMN binding at pH 2.0 strongly stabilizes the native state (although at 25°C, 8% of the molecules are molten globules) and holoflavodoxin experiences a less pronounced cold denaturation than the apo form. It is curious that the temperature dependencies of ΔG_1 and ΔG_2 make heat denaturation a three-state process but cold denaturation a simpler two-state process in which holoflavodoxin unfolds without molten globule accumulation. (Fig. 8 *B*).

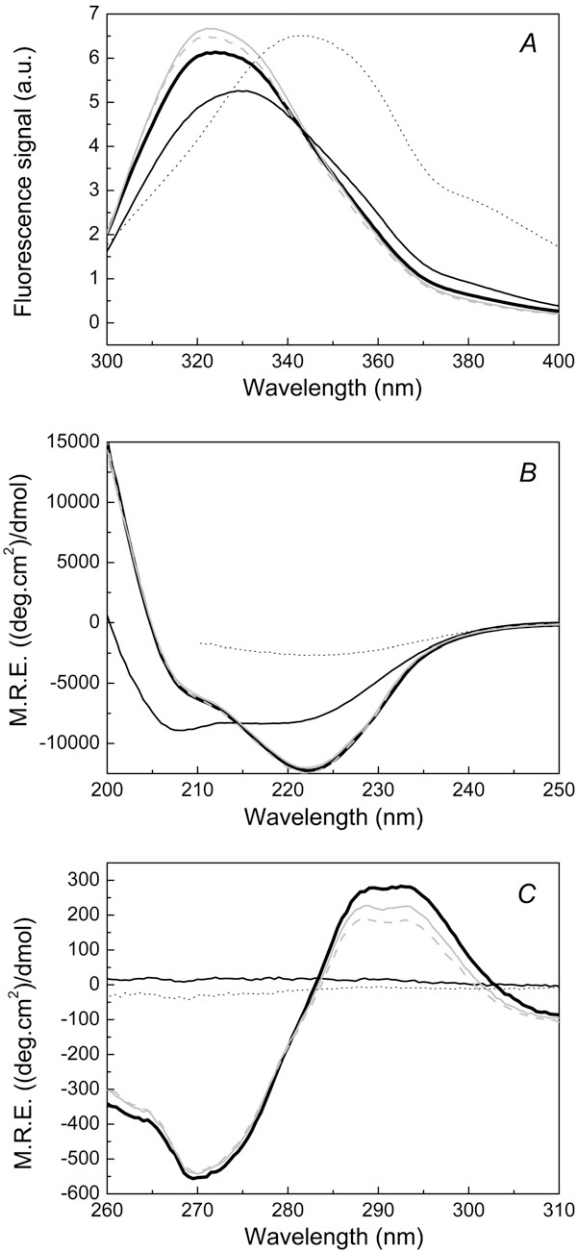

FIGURE 7 Spectroscopic characterization of holoflavodoxin at different pH values. (*A–C*) Fluorescence (*A*), far-UV CD (*B*), and near-UV CD spectra (*C*) of holoflavodoxin at 25°C and pH 2 (*thick black solid line*), pH 5 (*gray solid line*), and pH 7 (*gray dashed line*). The spectra of holoflavodoxin at pH 2 at 90°C (*dotted line*) and apoflavodoxin at pH 2 at 25°C (*thin black solid line*) are also shown for reference.

Fluctuations of the native state ensemble of *H. pylori* flavodoxin with pH

The native ensemble of proteins, i.e., the alternative conformations that are not far in stability from the native state under native solution conditions, is attracting much interest because it is increasingly clear that the ensemble is involved in the dynamics associated with protein function and that, on the other hand, it might be related to the occurrence of confor-

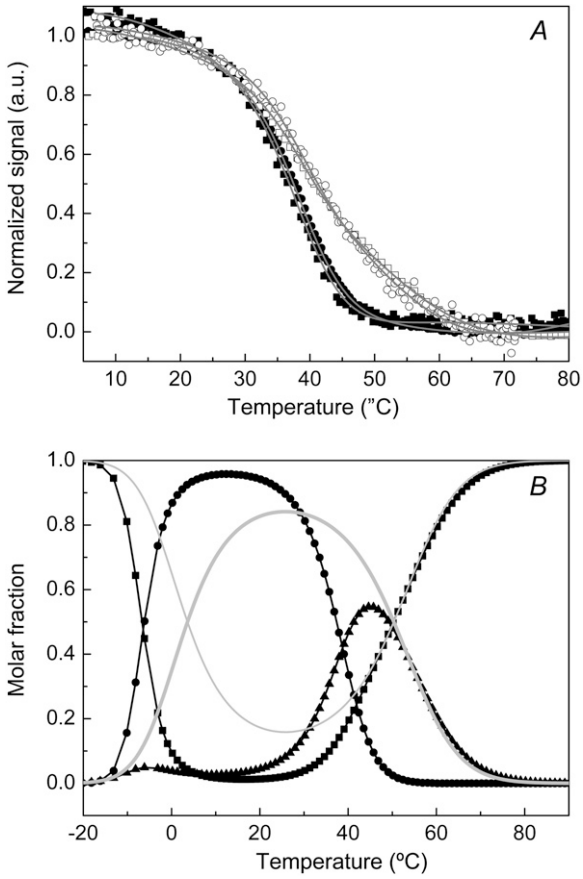

FIGURE 8 Holoflavodoxin thermal unfolding at pH 2.0. (*A*) Thermal unfolding of holoflavodoxin (equimolecular mixture of FMN and apoflavodoxin, 20 μM each) assessed by protein fluorescence (*open squares*), far-UV CD (*open circles*), near-UV CD (*solid squares*), and absorbance at 291 nm (*solid circles*). For a better comparison, the data were normalized so that the different curves run from roughly 0 to 1. The solid lines represent the global fit to a three-state unfolding model. (*B*) Populations of native (*circles*), molten globule (*triangles*), and thermally induced unfolded (*squares*) states. The populations of the different conformations in the absence of FMN are represented by thick gray lines for the molten globule and thin gray lines for the unfolded state.

mational diseases (2). Valuable information on native state ensembles has been obtained so far by NMR equilibrium studies (3–5). Here, we have used conventional protein stability techniques to characterize the native state ensemble of a model protein at acidic pH. Temperature, urea concentration, cofactor concentration, and pH markedly modify the relative stabilities of holoprotein, native apoprotein, and molten globule. On the other hand, the native ensemble of this protein at neutral and mildly basic pH has been characterized previously using similar techniques and was shown to include two partly unfolded intermediates (24). The picture that emerges from these analyses (Fig. 9) provides insight into the ensembles present as a function of pH. It has been pointed out that only conformations with free energies within 3–4 kcal/mol of the native-state free energy are likely to become significantly populated under native conditions and thus should be considered part of the native ensemble (2). At neutral and mildly acidic pH values, the native state ensemble of *H. pylori* apoflavodoxin is constituted by two partly unfolded intermediates plus the molten globule (Fig. 9). The more stable intermediate (24), whose structure is similar to that described for the single *Anabaena* apoflavodoxin thermal intermediate (6), is so close in energy to the native state that it becomes dominant upon small temperature increases. There is also strong evidence that it becomes the dominant conformation of a variety of partly unfolded point mutants (29,30), and that it appears to be related to the mechanism of FMN binding (21). The second intermediate, of lower stability, appears at higher temperatures, and little is known of its structure except that its helix content is low. The molten globule, with high helix content, is ~3 kcal/mol above the native state and represents the least stable intermediate in the native ensemble. Not surprisingly, it has not yet been observed at these pH values under either heat or mutational stress (point mutations). However, more drastic protein destabilization of *Anabaena* apoflavodoxin by removal of the terminal helix gives rise to the molten globule conformation (8). Only native apoflavodoxin can directly bind the cofactor, but the alternative conformations in the native ensemble are in equilibrium with native apoflavodoxin, and thus FMN drives them into the native state. Four partially unfolded forms (PUFs) of the homologous apoflavodoxin from *Azotobacter vinelandii* have been detected and studied by NMR (87). PUF 1 is very similar to the native state, PUF 2 corresponds to the more stable intermediate in *H. pylori* thermal unfolding, and PUF 4 is essentially an unfolded conformation. It is possible, but uncertain, that PUF 3 is related to the second thermal intermediate in *H. pylori* apoflavodoxin thermal unfolding, but none of these PUFs appear related to the molten globule. As the pH approaches 4.0, preferential proton binding to the molten globule reduces its energy gap with the native state,

TABLE 4 Thermal unfolding of flavodoxin at pH 2.0

	Holo ⇄ MG			MG ⇄ U			
	T_{m1} (°C)	ΔH_{m1} (kcal/mol)	ΔC_{P1} (kcal/(mol × K))	T_{m2} (°C)	ΔH_{m2} (kcal/mol)	ΔC_{P2} (kcal/(mol × K))	ΔG* (kcal/mol)
Apoflavodoxin[†]	–	–	–	50.4 ± 0.3	26.8 ± 0.8	1.09 ± 0.2	0.99 ± 0.07
Holoflavodoxin	38.8 ± 0.5	44 ± 1	1.5 ± 0.1	49.8 ± 2	23 ± 3	1.09[‡]	2.2 ± 0.4

*Global unfolding free energy (Holo↔U or MG↔U) at 25°C.
[†]Parameters obtained by global analysis of apoflavodoxin cold denaturation (data in Fig. 2).
[‡]ΔC_{P2} for holoflavodoxin was fixed to the $\Delta C_{P,MG\text{-}U}$ value of apoflavodoxin.

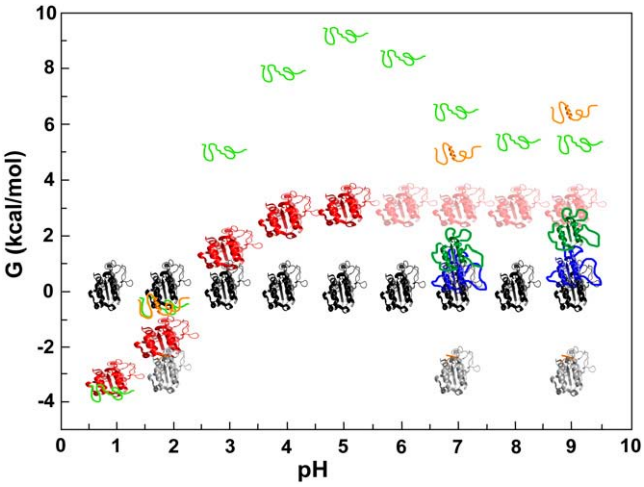

FIGURE 9 Energy landscape of *H. pylori* flavodoxin native state ensemble as a function of pH, showing the free energy along the pH axes (with $G = 0$ for native apoflavodoxin) of the different flavodoxin conformations that have been observed to become significantly populated. Native state apoflavodoxin is shown in black; molten globule in red; the more stable thermal intermediate observed at pH 7 and 9 in blue; the less stable thermal intermediate in dark green; the thermal unfolding state in orange (the different degree of unfolding proposed for these conformations in Cremades et al. (24) is schematically depicted); the urea-unfolded state in light green; and the flavodoxin/FMN complex in gray. The molten globule is in pale red in the pH 6–9 range to indicate that its energy is assumed to be that exhibited at pH 5. This assumption is based on the fact that the two histidine residues of the flavodoxin, responsible for the variations in protein stability in this pH region (25), are on the surface (21), and no large differences in histidine protonation are expected between the native and molten globule states. This is borne out by the fact that the molten globule is not observed in the thermal unfolding at neutral-basic pH, which indicates that it is less stable than the two thermal partially unfolded states.

and below pH 2.5, the molten globule is dominant. Even at pH 2.0, cofactor binding to the tiny fraction of native apoflavodoxin effectively shifts the equilibrium toward the native apoflavodoxin:FMN complex. The two intermediates that at neutral pH are closer to the native state than the molten globule appear to be destabilized at lower pH, and no longer populate upon heating.

It is clear that much information concerning protein function and dysfunction is confined in the details of the native state ensemble, and that stability differences between the native conformation and less stable, minor conformations of the ensemble may be more important than the overall stability of the native protein relative to the unfolded state (2,60,61). Indeed, partly folded intermediates, such as those shown here to constitute the native state ensemble of *H. pylori* apoflavodoxin, are thought to be critical intermediates involved in the onset of conformational diseases, including aggregation and subsequent fibril formation (47,88–91). Although NMR methods are very useful to detect and characterize the conformation of dominant species within the native state ensemble (3–5), conventional stability analysis can greatly help to understand the energetics of the ensembles and explain their fluctuations under changing solution conditions.

We acknowledge financial support from grants BFU2007-61476/BMC, from the Spanish Ministerio de Educación y Ciencia, and PM076/2006, from the Diputación General de Aragon, Spain. N.C. was supported by an FPU fellowship (Spain).

REFERENCES

1. Dobson, C. M. 2003. Protein folding and misfolding. *Nature*. 426:884–890.
2. Cremades, N., J. Sancho, and E. Freire. 2006. The native-state ensemble of proteins provides clues for folding, misfolding and function. *Trends Biochem. Sci.* 31:494–496.
3. Bai, Y., T. R. Sosnick, L. Mayne, and S. W. Englander. 1995. Protein folding intermediates: native-state hydrogen exchange. *Science*. 269:192–197.
4. Englander, S. W. 2000. Protein folding intermediates and pathways studied by hydrogen exchange. *Annu. Rev. Biophys. Biomol. Struct.* 29: 213–238.
5. Hilser, V. J., and E. Freire. 1996. Structure-based calculation of the equilibrium folding pathway of proteins. Correlation with hydrogen exchange protection factors. *J. Mol. Biol.* 262:756–772.
6. Campos, L. A., M. Bueno, J. Lopez-Llano, M. A. Jimenez, and J. Sancho. 2004. Structure of stable protein folding intermediates by equilibrium phi-analysis: the apoflavodoxin thermal intermediate. *J. Mol. Biol.* 344:239–255.
7. Ionescu, R. M., V. F. Smith, J. C. O'Neill, Jr., and C. R. Matthews. 2000. Multistate equilibrium unfolding of *Escherichia coli* dihydrofolate reductase: thermodynamic and spectroscopic description of the native, intermediate, and unfolded ensembles. *Biochemistry*. 39:9540–9550.
8. Lopez-Llano, J., L. A. Campos, M. Bueno, and J. Sancho. 2006. Equilibrium ϕ-analysis of a molten globule: the 1–149 apoflavodoxin fragment. *J. Mol. Biol.* 356:354–366.
9. Yan, S., G. Gawlak, J. Smith, L. Silver, A. Koide, and S. Koide. 2004. Conformational heterogeneity of an equilibrium folding intermediate quantified and mapped by scanning mutagenesis. *J. Mol. Biol.* 338: 811–825.
10. Ptitsyn, O. B., R. H. Pain, G. V. Semisotnov, E. Zerovnik, and O. I. Razgulyaev. 1990. Evidence for a molten globule state as a general intermediate in protein folding. *FEBS Lett.* 262:20–24.
11. Dill, K. A., and D. Shortle. 1991. Denatured states of proteins. *Annu. Rev. Biochem.* 60:795–825.
12. Bychkova, V. E., R. H. Pain, and O. B. Ptitsyn. 1988. The 'molten globule' state is involved in the translocation of proteins across membranes? *FEBS Lett.* 238:231–234.
13. van der Goot, F. G., J. H. Lakey, and F. Pattus. 1992. The molten globule intermediate for protein insertion or translocation through membranes. *Trends Cell Biol.* 2:343–348.
14. Ferrero, R. L., and A. Lee. 1991. The importance of urease in acid protection for the gastric-colonising bacteria *H. pylori* and *H. felis* sp. nov. *Microb. Ecol. Health Dis.* 4:121–134.
15. Marshall, B. J., and J. R. Warren. 1984. Unidentified curved bacilli in the stomach of patients with gastritis and peptic ulceration. *Lancet*. 1: 1311–1315.
16. Stingl, K., K. Altendorf, and E. P. Bakker. 2002. Acid survival of *Helicobacter pylori*: how does urease activity trigger cytoplasmic pH homeostasis? *Trends Microbiol.* 10:70–74.
17. Wen, Y., E. A. Marcus, U. Matrubutham, M. A. Gleeson, D. R. Scott, and G. Sachs. 2003. Acid-adaptive genes of *Helicobacter pylori*. *Infect. Immun.* 71:5921–5939.
18. Stingl, K., E. M. Uhlemann, R. Schmid, K. Altendorf, and E. P. Bakker. 2002. Energetics of *Helicobacter pylori* and its implications for the mechanism of urease-dependent acid tolerance at pH 1. *J. Bacteriol.* 184:3053–3060.
19. Sancho, J. 2006. Flavodoxins: sequence, folding, binding, function and beyond. *Cell. Mol. Life Sci.* 63:855–864.

20. St Maurice, M., N. Cremades, M. A. Croxen, G. Sisson, J. Sancho, and P. S. Hoffman. 2007. Flavodoxin:quinone reductase (FqrB): a redox partner of pyruvate:ferredoxin oxidoreductase that reversibly couples pyruvate oxidation to NADPH production in *Helicobacter pylori* and *Campylobacter jejuni*. *J. Bacteriol.* 189:4764–4773.
21. Martínez-Júlvez, M., N. Cremades, M. Bueno, I. Perez-Dorado, C. Maya, S. Cuesta-López, D. Prada, F. Falo, J. A. Hermoso, and J. Sancho. 2007. Common conformational changes in flavodoxins induced by FMN and anion binding: The structure of *Helicobacter pylori* apoflavodoxin. *Proteins.* 69:581–594.
22. Freigang, J., K. Diederichs, K. P. Schafer, W. Welte, and R. Paul. 2002. Crystal structure of oxidized flavodoxin, an essential protein in Helicobacter pylori. *Protein Sci.* 11:253–261.
23. Cremades, N., M. Bueno, M. Toja, and J. Sancho. 2005. Towards a new therapeutic target: *Helicobacter pylori* flavodoxin. *Biophys. Chem.* 115:267–276.
24. Cremades, N., A. Velazquez-Campoy, E. Freire, and J. Sancho. 2008. The flavodoxin from *Helicobacter pylori*: Structural determinants of thermostability and FMN cofactor binding. *Biochemistry.* 47:627–639.
25. Cremades, N., M. Bueno, J. L. Neira, A. Velazquez-Campoy, and J. Sancho. 2008. Conformational stability of *Helicobacter pylori* flavodoxin. Fit to function at pH 5. *J. Biol. Chem.* 283:2883–2895.
26. Genzor, C. G., A. Beldarrain, C. Gomez-Moreno, J. L. Lopez-Lacomba, M. Cortijo, and J. Sancho. 1996. Conformational stability of apoflavodoxin. *Protein Sci.* 5:1376–1388.
27. Maldonado, S., G. M. Langdon, M. A. Jimenez, and J. Sancho. 1998. Cooperative stabilization of a molten globule apoflavodoxin fragment. *Biochemistry.* 37:10589–10596.
28. Whitten, S. T., A. J. Kurtz, M. S. Pometun, A. J. Wand, and V. J. Hilser. 2006. Revealing the nature of the native state ensemble through cold denaturation. *Biochemistry.* 45:10163–10174.
29. Bueno, M., N. Cremades, J.L. Neira, and J. Sancho. 2006. Filling small, empty protein cavities: structural and energetic consequences. *J. Mol. Biol.* 358:701–712.
30. Lopez-Llano, J., S. Maldonado, M. Bueno, A. Lostao, M. A. Jimenez, M. P. Lillo, and J. Sancho. 2004. The long and short flavodoxins: I. The role of the differentiating loop in apoflavodoxin structure and FMN binding. *J. Biol. Chem.* 279:47177–47183.
31. Edmondson, D. E., and G. Tollin. 1971. Chemical and physical characterization of the Shethna flavoprotein and apoprotein and kinetics and thermodynamics of flavin analog binding to the apoprotein. *Biochemistry.* 10:124–132.
32. Myers, J. K., C. N. Pace, and J. M. Scholtz. 1995. Denaturant *m* values and heat capacity changes: relation to changes in accessible surface areas of protein unfolding. *Protein Sci.* 4:2138–2148.
33. Santoro, M. M., and D. W. Bolen. 1988. Unfolding free energy changes determined by the linear extrapolation method. 1. Unfolding of phenylmethanesulfonyl α-chymotrypsin using different denaturants. *Biochemistry.* 27:8063–8068.
34. Bollen, Y. J., I. E. Sanchez, and C. P. van Mierlo. 2004. Formation of on- and off-pathway intermediates in the folding kinetics of *Azotobacter vinelandii* apoflavodoxin. *Biochemistry.* 43:10475–10489.
35. Schellman, J. A. 1987. The thermodynamic stability of proteins. *Annu. Rev. Biophys. Chem.* 16:115–137.
36. Chen, B. L., and J. A. Schellman. 1989. Low-temperature unfolding of a mutant of phage T4 lysozyme. 1. Equilibrium studies. *Biochemistry.* 28:685–691.
37. Agashe, V. R., and J. B. Udgaonkar. 1995. Thermodynamics of denaturation of barstar: evidence for cold denaturation and evaluation of the interaction with guanidine hydrochloride. *Biochemistry.* 34:3286–3299.
38. Tanford, C. 1970. Protein denaturation. C. Theoretical models for the mechanism of denaturation. *Adv. Protein Chem.* 24:1–95.
39. Makhatadze, G. I., and P. L. Privalov. 1992. Protein interactions with urea and guanidinium chloride. A calorimetric study. *J. Mol. Biol.* 226: 491–505.
40. Sasahara, K., P. McPhie, and A. P. Minton. 2003. Effect of dextran on protein stability and conformation attributed to macromolecular crowding. *J. Mol. Biol.* 326:1227–1237.
41. Minton, A. P. 2000. Effect of a concentrated ''inert'' macromolecular cosolute on the stability of a globular protein with respect to denaturation by heat and by chaotropes: a statistical-thermodynamic model. *Biophys. J.* 78:101–109.
42. Ogston, A. G. 1958. The spaces in a uniform random suspensions of fibres. *Trans. Faraday Soc.* 54:1754–1757.
43. Laurent, T. C., and J. Killander. 1964. A theory of gel filtration and its experimental verification. *J. Chromatogr.* 14:317–330.
44. Rivas, G., J. A. Fernandez, and A. P. Minton. 1999. Direct observation of the self-association of dilute proteins in the presence of inert macromolecules at high concentration via tracer sedimentation equilibrium: theory, experiment, and biological significance. *Biochemistry.* 38:9379–9388.
45. Hammarstrom, P., M. Persson, P. O. Freskgard, L. G. Martensson, D. Andersson, B. H. Jonsson, and U. Carlsson. 1999. Structural mapping of an aggregation nucleation site in a molten globule intermediate. *J. Biol. Chem.* 274:32897–32903.
46. Martin, J., T. Langer, R. Boteva, A. Schramel, A. L. Horwich, and F. U. Hartl. 1991. Chaperonin-mediated protein folding at the surface of groEL through a 'molten globule'-like intermediate. *Nature.* 352:36–42.
47. Booth, D. R., M. Sunde, V. Bellotti, C. V. Robinson, W. L. Hutchinson, P. E. Fraser, P. N. Hawkins, C. M. Dobson, S. E. Radford, C. C. Blake, and M. B. Pepys. 1997. Instability, unfolding and aggregation of human lysozyme variants underlying amyloid fibrillogenesis. *Nature.* 385:787–793.
48. Pace, C. N., B. A. Shirley, and J. A. Thomson. 1989. Measuring the conformational stability of a protein. *In* Protein Structure: A Practical Approach. T. E. Creighton, editor. Oxford University Press, Oxford, United Kingdom. 311–330.
49. Zweifel, M. E., and D. Barrick. 2002. Relationships between the temperature dependence of solvent denaturation and the denaturant dependence of protein stability curves. *Biophys. Chem.* 101–102:221–237.
50. Robertson, A. D., and K. P. Murphy. 1997. Protein structure and the energetics of protein stability. *Chem. Rev.* 97:1251–1268.
51. Li, H., A. D. Robertson, and J. H. Jensen. 2005. Very fast empirical prediction and rationalization of protein pKa values. *Proteins.* 61:704–721.
52. Palleros, D. R., L. Shi, K. L. Reid, and A. L. Fink. 1993. Three-state denaturation of DnaK induced by guanidine hydrochloride. Evidence for an expandable intermediate. *Biochemistry.* 32:4314–4321.
53. Ptitsyn, O. B. 1992. The molten globule state. *In* Protein Folding. T. E. Creighton, editor. W. H. Freeman, New York. 243–300.
54. Zimmerman, S. B., and A. P. Minton. 1993. Macromolecular crowding: biochemical, biophysical, and physiological consequences. *Annu. Rev. Biophys. Biomol. Struct.* 22:27–65.
55. Minton, A. P., and J. Wilf. 1981. Effect of macromolecular crowding upon the structure and function of an enzyme: glyceraldehyde-3-phosphate dehydrogenase. *Biochemistry.* 20:4821–4826.
56. Lebowitz, J. L., E. Hefland, and E. Paestgaard. 1965. Scaled particle theory of fluids mixtures. *J. Chem. Phys.* 43:774–779.
57. Minton, A. P. 1981. Excluded volume as a determinant of macromolecular structure and reactivity. *Biopolymers.* 20:2093–2120.
58. Berg, O. G. 1990. The influence of macromolecular crowding on thermodynamic activity: solubility and dimerization constants for spherical and dumbbell-shaped molecules in a hard-sphere mixture. *Biopolymers.* 30:1027–1037.
59. Stagg, L., S. Q. Zhang, M. S. Cheung, and P. Wittung-Stafshede. 2007. Molecular crowding enhances native structure and stability of α/β protein flavodoxin. *Proc. Natl. Acad. Sci. USA.* 104:18976–18981.
60. Sancho, J., M. Bueno, L. A. Campos, J. Fernandez-Recio, M. P. Irun, J. Lopez-Llano, C. Machicado, I. Pedroso, and M. Toja. 2002. The 'relevant' stability of proteins with equilibrium intermediates. *ScientificWorldJournal.* 2:1209–1215.

61. Campos, L. A., M. M. Garcia-Mira, R. Godoy-Ruiz, J. M. Sanchez-Ruiz, and J. Sancho. 2004. Do proteins always benefit from a stability increase? Relevant and residual stabilisation in a three-state protein by charge optimisation. *J. Mol. Biol.* 344:223–237.

62. Crowe, J. H., F. A. Hoekstra, and J. M. Crowe. 1992. Anhydrobiosis. *Annu. Rev. Physiol.* 54:579–599.

63. Yancey, P. H., M. E. Clark, S. C. Hand, R. D. Bowlus, and G. N. Somero. 1982. Living with water stress: evolution of osmolyte systems. *Science.* 217:1214–1222.

64. Garcia-Perez, A., and M. B. Burg. 1991. Renal medullary organic osmolytes. *Physiol. Rev.* 71:1081–1115.

65. Singer, M. A., and S. Lindquist. 1998. Multiple effects of trehalose on protein folding in vitro and in vivo. *Mol. Cell.* 1:639–648.

66. Hochachka, P. W., and G. N. Somero. 2002. Biochemical Adaptation: Mechanism and Process in Physiological Evolution. Oxford University Press, New York.

67. Liu, Y., and D. W. Bolen. 1995. The peptide backbone plays a dominant role in protein stabilization by naturally occurring osmolytes. *Biochemistry.* 34:12884–12891.

68. Arakawa, T., R. Bhat, and S. N. Timasheff. 1990. Preferential interactions determine protein solubility in three-component solutions: the MgCl2 system. *Biochemistry.* 29:1914–1923.

69. Bolen, D. W., and I. V. Baskakov. 2001. The osmophobic effect: natural selection of a thermodynamic force in protein folding. *J. Mol. Biol.* 310:955–963.

70. Lee, J. C., K. Gekko, and S. N. Timasheff. 1979. Measurements of preferential solvent interactions by densimetric techniques. *Methods Enzymol.* 61:26–49.

71. Qu, Y., C. L. Bolen, and D. W. Bolen. 1998. Osmolyte-driven contraction of a random coil protein. *Proc. Natl. Acad. Sci. USA.* 95:9268–9273.

72. Auton, M., A. C. Ferreon, and D. W. Bolen. 2006. Metrics that differentiate the origins of osmolyte effects on protein stability: a test of the surface tension proposal. *J. Mol. Biol.* 361:983–992.

73. Lee, J. C., and S. N. Timasheff. 1981. The stabilization of proteins by sucrose. *J. Biol. Chem.* 256:7193–7201.

74. Kaushik, J. K., and R. Bhat. 2003. Why is trehalose an exceptional protein stabilizer? An analysis of the thermal stability of proteins in the presence of the compatible osmolyte trehalose. *J. Biol. Chem.* 278:26458–26465.

75. Lin, T. Y., and S. N. Timasheff. 1996. On the role of surface tension in the stabilization of globular proteins. *Protein Sci.* 5:372–381.

76. Saunders, A. J., P. R. Davis-Searles, D. L. Allen, G. J. Pielak, and D. A. Erie. 2000. Osmolyte-induced changes in protein conformational equilibria. *Biopolymers.* 53:293–307.

77. Schellman, J. A. 2003. Protein stability in mixed solvents: a balance of contact interaction and excluded volume. *Biophys. J.* 85:108–125.

78. Davis-Searles, P. R., A. S. Morar, A. J. Saunders, D. A. Erie, and G. J. Pielak. 1998. Sugar-induced molten-globule model. *Biochemistry.* 37:17048–17053.

79. Morar, A. S., A. Olteanu, G. B. Young, and G. J. Pielak. 2001. Solvent-induced collapse of α-synuclein and acid-denatured cytochrome *c*. *Protein Sci.* 10:2195–2199.

80. Yancey, P. H., and G. N. Somero. 1979. Counteraction of urea destabilization of protein structure by methylamine osmoregulatory compounds of elasmobranch fishes. *Biochem. J.* 183:317–323.

81. Wang, A., and D. W. Bolen. 1997. A naturally occurring protective system in urea-rich cells: mechanism of osmolyte protection of proteins against urea denaturation. *Biochemistry.* 36:9101–9108.

82. Colombo, M. F., D. C. Rau, and V. A. Parsegian. 1992. Protein solvation in allosteric regulation: a water effect on hemoglobin. *Science.* 256:655–659.

83. Pace, C. N., and T. McGrath. 1980. Substrate stabilization of lysozyme to thermal and guanidine hydrochloride denaturation. *J. Biol. Chem.* 255:3862–3865.

84. Brandts, J. F., and L. N. Lin. 1990. Study of strong to ultratight protein interactions using differential scanning calorimetry. *Biochemistry.* 29: 6927–6940.

85. Straume, M., and E. Freire. 1992. Two-dimensional differential scanning calorimetry: simultaneous resolution of intrinsic protein structural energetics and ligand binding interactions by global linkage analysis. *Anal. Biochem.* 203:259–268.

86. Campos, L. A., and J. Sancho. 2006. Native-specific stabilization of flavodoxin by the FMN cofactor: structural and thermodynamical explanation. *Proteins.* 63:581–594.

87. Bollen, Y. J., M. B. Kamphuis, and C. P. van Mierlo. 2006. The folding energy landscape of apoflavodoxin is rugged: hydrogen exchange reveals nonproductive misfolded intermediates. *Proc. Natl. Acad. Sci. USA.* 103:4095–4100.

88. Khurana, R., J. R. Gillespie, A. Talapatra, L. J. Minert, C. Ionescu-Zanetti, I. Millett, and A. L. Fink. 2001. Partially folded intermediates as critical precursors of light chain amyloid fibrils and amorphous aggregates. *Biochemistry.* 40:3525–3535.

89. Nielsen, L., R. Khurana, A. Coats, S. Frokjaer, J. Brange, S. Vyas, V. N. Uversky, and A. L. Fink. 2001. Effect of environmental factors on the kinetics of insulin fibril formation: elucidation of the molecular mechanism. *Biochemistry.* 40:6036–6046.

90. Ahmad, A., I. S. Millett, S. Doniach, V. N. Uversky, and A. L. Fink. 2003. Partially folded intermediates in insulin fibrillation. *Biochemistry.* 42:11404–11416.

91. Kirkitadze, M. D., M. M. Condron, and D. B. Teplow. 2001. Identification and characterization of key kinetic intermediates in amyloid beta-protein fibrillogenesis. *J. Mol. Biol.* 312:1103–1119.